Inorg. Chem. **2002**, *41*, 4987–4989

Dynamic Behavior in Diplatinum Metalloreceptors

Andrew J. Baer,[†] Bryan D. Koivisto,[†] Adrien P. Côté,[†] Nicholas J. Taylor,[†] Garry S. Hanan,*[,†] Hélène Nierengarten,[‡] and Alain Van Dorsselaer[‡]

Department of Chemistry, University of Waterloo, 200 University Avenue West, Waterloo, Ontario N2L 3G1, Canada, and UMR 7509, LSMBO-ECPM, 67087 Strasbourg, France

Received April 28, 2002

Diplatinum metalloreceptors *anti*-**4a** and *anti*-**4b** exhibit dynamic behavior in solution that is modified by anion binding. An X-ray crystal structure determination of *anti*-**4a** supports its proposed solution structure.

The ligand-to-metal dative bond has been used extensively to assemble well-defined and robust supramolecular structures.[1] The assembly of predictable structures depends to a large extent on the lability of the metal−ligand interaction, in which "error-checking" in the assembly process leads to the desired thermodynamic product.[2] While rigid assemblies are usually the most desired structures, more flexible assemblies may favor the binding of guest molecules into metalloreceptors, such as found for the induced-fit mechanism of enzymes.[3] This approach would favor weak interactions for guest binding, such as hydrogen bonding, $\pi-\pi$ interactions, and hydrophobic/hydrophilic interactions. Metalloreceptors may bind substrate through their primary coordination sphere (i.e., metal binding to substrate), their secondary coordination sphere (i.e., ligand binding to substrate), or a combination of both coordination spheres. Binding only through the secondary coordination sphere has been explored considerably less than the other modes.[4]

The metalloreceptors require organic ligands containing three essential parts: metal-binding units, a rigid spacer, and hydrogen-bonding groups (Figure 1a). The spacers hold the metal-binding units apart such that intramolecular complexation of one metal ion is not possible. When two or more ligands are brought together by two metal ions, a pocket is formed, complete with sites for hydrogen-bonding interactions.[5] For example, a large, closed structure may be assembled by using metal ions with trans square-planar coordination geometry (Figure 1b).

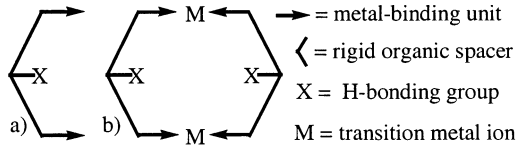

Figure 1. (a) Representation of organic ligand and (b) two ligands assembled around two trans square-planar metal ions.

Chart 1. Isomeric *N*,*N*′-Bis(pyridyl)-2,6-pyridinedicarboxamides **1** and **2** and the Isophthalamide **3**

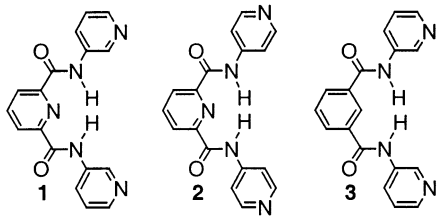

Herein we apply this strategy to the synthesis of a new series of *dynamic* diplatinum metallomacrocycles and present their NMR behavior and host−guest chemistry based on interactions with the secondary coordination sphere of the metalloreceptors.

The appropriate ligand framework is available in the diamidopyridine motif of *N*,*N*′-bis(pyridin-3-yl)-2,6-pyridinedicarboxamide (**1**), which is similar to a ligand (**2**) used in anion[6] and dicarboxamide[7] receptors (Chart 1). The central pyridinedicarboxamide motif in **1** and **2** has previously been

* Author to whom correspondence should be addressed. E-mail: ghanan@uwaterloo.ca.
† University of Waterloo.
‡ LSMBO-ECPM.

(1) Holliday, B. J.; Mirkin, C. A. *Angew. Chem., Int. Ed.* **2001**, *40*, 2022. Linton, B.; Hamilton, A. D. *Chem. Rev.* **1997**, *97*, 1669. Fujita, M.; Ogura, K. *Coord. Chem. Rev.* **1996**, *148*, 249.
(2) Lehn, J.-M. *Science* **2002**, *295*, 2400. Lehn, J.-M. *Supramolecular Chemistry—Concepts and Perspectives*; VCH: Weinheim, 1995.
(3) Fersht, A. R. *Enzyme Structure and Mechanism*, 2nd ed; Freeman: New York, 1985.
(4) Loeb, S. J. In *Comprehensive Supramolecular Chemistry*; Atwood, J. L., Davies, J. E. D., MacNicol, D. D., Vogtle F., Lehn, J.-M., Eds.; Pergamon: Oxford, 1996. Colquhoun, H. M.; Stoddart, J. F.; Williams, D. J. *Angew. Chem., Int. Ed. Engl.* **1986**, *25*, 487.
(5) Monometallic receptors capable of hydrogen-bonding interactions have been described, e.g.: Kickham, J. E.; Loeb, S. J.; Murphy, S. L. *J. Am. Chem. Soc.* **1993**, *115*, 7031. Goodman, M. S.; Weiss, J.; Hamilton, A. D. *Tetrahedron Lett.* **1994**, *35*, 8943. Goodman, M. S.; Hamilton, A. D.; Weiss, J. *J. Am. Chem. Soc.* **1995**, *117*, 8447. Goodman, M. S.; Jubian, V.; Hamilton, A. D. *Tetrahedron Lett.* **1995**, *36*, 2551. Huc, I.; Krische, M. J.; Funeriu, D. P.; Lehn, J.-M. *Eur. J. Inorg. Chem.* **1999**, 1415.
(6) Sun, S. S.; Lees, A. J. *Chem. Commun.* **2000**, 1687.
(7) Jeong, K. S.; Cho, Y. L.; Chang, S. Y.; Park, T. Y.; Song, J. U. *J. Org. Chem.* **1999**, *64*, 9459. Jeong, K. S.; Lee, J. W.; Park, T. Y.; Chang, S. Y. *Chem. Commun.* **1999**, 2069.

10.1021/ic0256819 CCC: $22.00
Published on Web 09/11/2002

Chart 2. Two Possible Isomers in the Synthesis of Metallomacrocycles *cis*-$Pt_2(\mathbf{1})_2(PR_3)_4^{4+}$: *syn*-**4** and *anti*-**4**[a]

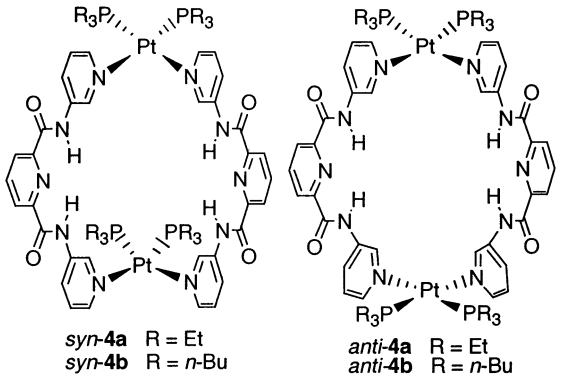

[a] Syn or anti with respect to the $Pt(PR_3)_2$ moieties.

shown to enforce inwardly directed amide N−H's and to bind H-bond acceptor groups.[8] The 3-pyridyl motif of **1** should also allow an open cavity to be formed with cis coordination to metal ions, suitable for facile entry of guest molecules to the H-bonding donors on the pyridinedicarboxamide core. Recently, gold metallomacrocycles of **3** have been shown to possess interesting structural features; however, no host−guest chemistry was reported.[9]

The treatment of *cis*-$PtCl_2(PR_3)_2$ complexes (R = Et, *n*-Bu) with 2 equiv of $AgPF_6$ followed by 1 equiv of **1** gave the platinum macrocycles *cis*-$Pt_2(\mathbf{1})_2(PR_3)_4^{4+}$ (R = Et (*anti*-**4a**), Bu (*anti*-**4b**)) as their PF_6 salts in 79% and 82% yield, respectively (Chart 2).[10] The diphosphino platinum moieties may have syn or anti orientations in the complexes, in which the isomers differ only by a rotation about the amido-N to 3-pyridyl-C bond (Chart 2).

At 298 K in DMSO-d_6, the ^{1}H, ^{31}P, and ^{13}C NMR spectra of the complexes clearly indicate the formation of a single symmetric species, showing typical shifts due to metal complexation for the proton resonances of **1**. However, distinguishing between syn or anti was not possible based on ^{1}H NMR in DMSO-d_6 and ES-MS studies, even though the latter confirmed the assembly of a 2 + 2 (two ligands and two metal ions) metalloreceptor.

Three experiments were undertaken in order to assign the complexes as syn or anti. First, a series of ^{1}H NMR spectra were recorded in CD_3CN over the range 238−298 K. As the temperature was lowered from 298 to 250 K, the resonances showed significant broadening along with the gradual appearance of two new sets of resonances. Below 250 K, the two new sets of resonances become increasingly distinct and are sharp and distinguishable by 238 K, indicating that a dynamic process is occurring on the NMR time scale.[11] The behavior observed in the ^{1}H NMR spectra

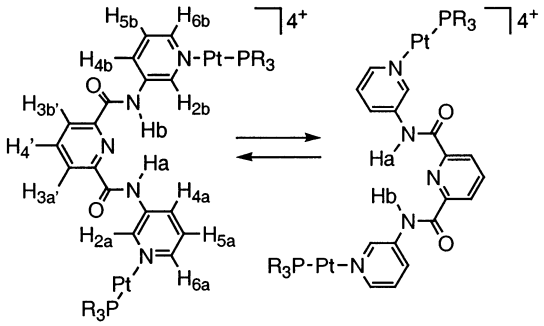

Figure 2. The proposed dynamic behavior of the metallomacrocycles. Two PR_3 ligands and one ligand **1** have been omitted for clarity.

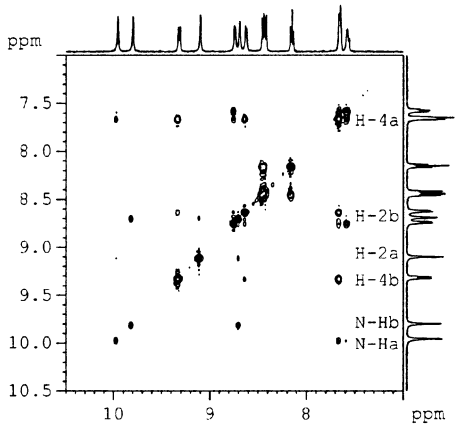

Figure 3. The ROESY spectrum of macrocycle *anti*-**4b** in CD_2Cl_2 at 233 K.

is consistent with the platinum metal centers exchanging between two different orientations (Figure 2).

Second, a line shape analysis of the temperature dependence of the ^{1}H spectra of complexes **4** in CD_3CN was performed to determine the energy barrier to the rotation of the outer pyridine rings.[12] From these calculations, the energy barrier was found to be 29.1 ± 3.8 and 28.4 ± 3.9 kJ/mol for *anti*-**4a** and *anti*-**4b**, respectively. The relatively low energy barrier for the interconversion of the Pt centers suggests that no bond breaking and forming occurs during this process. The robust nature of the metal−ligand bonds in the diplatinum metalloreceptors differs from recently published results for tripalladium metalloreceptors, in which an equilibrium of species exists.[13]

Third, the ROESY spectra of the metallomacrocycles were measured in CD_2Cl_2 at 233 K, and they show NOE signals between the proton resonances N−Ha and H-4a, and between N−Hb and H-2b (Figure 3). The signals are consistent with either of the structures shown in Figure 2. The absence of NOE signals between the amide protons and H-3a′ and H-3b′ supports the arrangement of the pyridinedicarboxamide motif as that depicted in Figure 2.[8] Upon warming to room temperature, the 13 ^{1}H NMR resonances collapse back to seven, consistent with the macrocycle alternating between the two orientations rapidly on the NMR time-scale.

The final confirmation of the bonding geometry at each Pt center came from the X-ray crystal structure of *anti*-**4a**.[14]

(8) Fredericks, J. R.; Hamilton, A. D. In *Comprehensive Supramolecular Chemistry*; Atwood, J. L., Davies, J. E. D., MacNicol, D. D., Vogtle, F., Lehn, J.-M., Eds.; Pergamon: Oxford, 1996.
(9) Qin, Z. Q.; Jennings, M. C.; Puddephatt, R. J. *Chem. Commun.* **2002**, 354. Qin, Z. Q.; Jennings, M. C.; Puddephatt, R. J. *Chem. Eur. J.* **2002**, *8*, 735.
(10) All new compounds were characterized by ^{1}H, ^{13}C, and ^{31}P NMR, ES-MS, and elemental analysis.
(11) Pons, M.; Millet, O. *Prog. Nucl. Magn. Reson. Spectrosc.* **2001**, *38*, 267.
(12) Line shape analyses were calculated using the program "MEXICO" by Alex Bain, McMaster University.
(13) Hiraoka, S.; Fujita, M. *J. Am. Chem. Soc.* **1999**, *121*, 10239.

Thus, *anti*-**4a** is clearly not symmetric in the solid state, and the assignment of the anti conformation is verified. The coordination planes of the platinum metal centers are at 74° relative to one another, leaving the binding pocket half-open. A PF_6^- anion occupies the central cavity, although $^{31}P\{^1H\}$ NMR indicates only one PF_6^- environment, suggesting relatively weak binding in solution.[15]

The Pt−N bond lengths vary from 2.071(8) to 2.110(8) Å, whereas the Pt−P bond lengths vary slightly less, from 2.256(3) to 2.283(3) Å. The (pyridine)N−Pt−N(pyridine) angles (Pt1 = 81.7°, Pt2 = 82.3°) are similar, although somewhat different angles are found for the $Et_3P-Pt-PEt_3$ environment (Pt1 = 98.84°, Pt2 = 95.82°). The shortest NH-to-F contacts are 3.100 Å (N18−F32) and 3.071 Å (N7−F32) with the PF_6 lying closer to Pt2 (F31−Pt2 = 3.292 Å) than Pt1 (F34−Pt1 = 4.963 Å). Both of the ligands **1** found in *anti*-**4a** show deviations from planarity of the outer pyridine rings relative to the central pyridinedicarboxamide; however, their internal bond lengths and bond angles are as expected for pyridine rings. Thus, the X-ray crystal structure of *anti*-**4a** is consistent with the NMR data obtained in CD_3CN, clearly demonstrating two distinct environments for the Pt centers.

The treatment of *anti*-**4a** and *anti*-**4b** with $(n\text{-Bu})_4NBF_4$ in CD_3CN led to strong BF_4 binding as compared to a recently described metalloreceptor (Figure 5).[16,17] More importantly, the binding of BF_4 also alters the dynamic behavior of the metalloreceptors. In Figure 5, the point of inflection for anion binding occurs near 1 equiv of anion added per 4 equiv of PF_6 present in the complexes. A Job plot verified the 1:1 anion-to-metalloreceptor stoichiometry. This tapers off as the number of equivalents reaches a 1:1 mixture of BF_4 and PF_6 anions (4 equiv of guest).

The difference in BF_4 binding constants is related to the difference in the size of the phosphine R groups. The *n*-butyl phosphines in *anti*-**4b** are more sterically encumbering than the ethyl phosphines in *anti*-**4a** (cf., Figure 4), which affects anion access to the metalloreceptor core. The fact that relatively strong anion binding persists suggests that access to the metalloreceptor core is not fully blocked and that electrostatic interaction between the host and guest is the driving force for binding.[18]

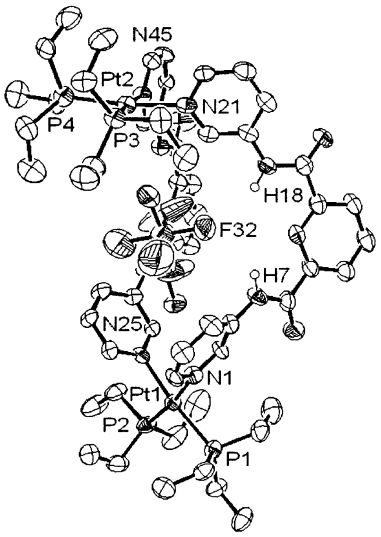

Figure 4. The single-crystal X-ray structure of metallomacrocycle *anti*-**4a** [*cis*-$Pt_2(\mathbf{1})_2(PEt_3)_4][PF_6]_4$ with Pt, P, and N labeled. Three PF_6 anions and the solvent of crystallization have been omitted for clarity. One PF_6 anion is bound in the central pocket.

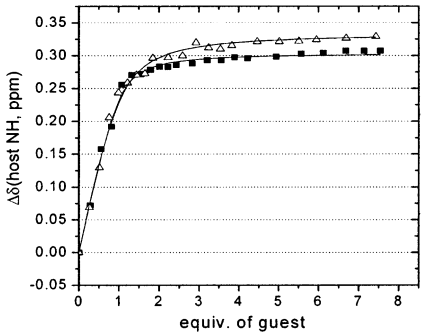

Figure 5. Plot of $\Delta\delta$ in ppm for the NH protons of metallomacrocycles *anti*-**4a** and *anti*-**4b** upon treatment with $(n\text{-Bu})_4NBF_4$ in CD_3CN at 298 K: (■) *anti*-**4a**; (△) *anti*-**4b**.

The variable temperature ^1H NMR spectra of *anti*-**4a** and *anti*-**4b** in CD_3CN in the presence of an equimolar amount of PF_6 and BF_4 show a dramatic change in the energy barrier for the "flipping" motion of the external pyridines. The new values, 50.2 ± 0.8 and 44.7 ± 1.0 kJ/mol for *anti*-**4a** and *anti*-**4b**, respectively, clearly indicate that guest binding has altered the dynamic behavior of the macrocycles to different extents for PEt_3 (*anti*-**4a**) vs $P(n\text{-Bu})_3$ (*anti*-**4b**). This suggests that fine control of the dynamic behavior of metalloreceptors may be possible.

We are currently exploring the dynamic behavior of the Pt metalloreceptors in the presence of other anions with the aim of using these metalloreceptors as hosts for neutral organic guests.

Acknowledgment. We thank the NSERC, the Research Corporation, the Province of Ontario, and the Davies Charitable Foundation for financial support.

Supporting Information Available: Experimental procedures for **1**, *anti*-**4a**, and *anti*-**4b**, VT-NMR spectra for *anti*-**4a** and *anti*-**4b**, and crystallographic data for *anti*-**4a**. This material is available free of charge via the Internet at http://pubs.acs.org.

IC0256819

(14) X-ray quality crystals of *anti*-**4a** were grown by slow evaporation of a $CH_3CN/CH_3COCH_3/CH_2Cl_2/CHCl_3$ solvent mixture. Crystal data for $C_{131}H_{198}Cl_9F_{48}N_{21}O_{11}P_{16}Pt_4$ were collected on a Bruker APEX at 150(1) K using Mo Kα radiation (λ = 0.71073 Å); reflections measured, 33704; unique data, 23767; M = 5104.53, monoclinic, space group $P2(1)/n$, a = 16.2383(14) Å, b = 31.882(3) Å, c = 38.187(3) Å, β = 90.158(2)°, V = 19769(3) Å^3, Z = 4, D_{obsd} = 1.715 g cm^{-3}, μ(Mo Kα) = 3.308 mm^{-1}, R1 [$I > 2\sigma(I)$] = 0.0864, wR2 (all unique data) = 0.1418.

(15) Beer, P. D.; Gale, P. A. *Angew. Chem., Int. Ed.* **2001**, *40*, 486.

(16) Bondy, C. R.; Gale, P. A.; Loeb, S. J. *Chem. Commun.* **2001**, 729. Strong anion binding was also observed in ref 6, although in a less competitive solvent, CH_2Cl_2.

(17) Binding constants were calculated using the program "EQ-NMR"; by ^1H NMR, *anti*-**4a**, K = 7100 ± 800 M^{-1}; *anti*-**4b**, K = 3400 ± 400 M^{-1}; and ^{19}F NMR, *anti*-**4a**, K = 7700 ± 400 M^{-1}; *anti*-**4b**, K = 3000 ± 250 M^{-1}; see: Hynes, M. J. *J. Chem. Soc., Dalton Trans.* **1993**, 311.

(18) No BF_4 binding was observed in the titration of ligand **1** with $TBABF_4$.